



Research

Cite this article: Sharma PP, Tarazona OA, Lopez DH, Schwager EE, Cohn MJ, Wheeler WC, Extavour CG. 2015 A conserved genetic mechanism specifies deutocerebral appendage identity in insects and arachnids. *Proc. R. Soc. B* **282**: 20150698.
<http://dx.doi.org/10.1098/rspb.2015.0698>

Received: 26 March 2015

Accepted: 16 April 2015

Subject Areas:

evolution, developmental biology

Keywords:

Arthropoda, deutocerebrum, antenna, chelicera, opiliones, serial homology

Author for correspondence:

Prashant P. Sharma

e-mail: psharma@amnh.org

Electronic supplementary material is available at <http://dx.doi.org/10.1098/rspb.2015.0698> or via <http://rspb.royalsocietypublishing.org>.

A conserved genetic mechanism specifies deutocerebral appendage identity in insects and arachnids

Prashant P. Sharma¹, Oscar A. Tarazona², Davys H. Lopez^{2,3}, Evelyn E. Schwager⁴, Martin J. Cohn², Ward C. Wheeler¹ and Cassandra G. Extavour³

¹Division of Invertebrate Zoology, American Museum of Natural History, Central Park West at 79th Street, New York, NY 10024, USA

²Department of Biology, University of Florida, Gainesville, FL 32611, USA

³Department of Organismic and Evolutionary Biology, Harvard University, Cambridge, MA 02138, USA

⁴Department of Biological and Medical Sciences, Oxford Brookes University, Oxford OX3 0BP, UK

The segmental architecture of the arthropod head is one of the most controversial topics in the evolutionary developmental biology of arthropods. The deutocerebral (second) segment of the head is putatively homologous across Arthropoda, as inferred from the segmental distribution of the tripartite brain and the absence of Hox gene expression of this anterior-most, appendage-bearing segment. While this homology statement implies a putative common mechanism for differentiation of deutocerebral appendages across arthropods, experimental data for deutocerebral appendage fate specification are limited to winged insects. Mandibulates (hexapods, crustaceans and myriapods) bear a characteristic pair of antennae on the deutocerebral segment, whereas chelicerates (e.g. spiders, scorpions, harvestmen) bear the eponymous chelicerae. In such hexapods as the fruit fly, *Drosophila melanogaster*, and the cricket, *Gryllus bimaculatus*, cephalic appendages are differentiated from the thoracic appendages (legs) by the activity of the appendage patterning gene *homothorax* (*hth*). Here we show that embryonic RNA interference against *hth* in the harvestman *Phalangium opilio* results in homeotic chelicera-to-leg transformations, and also in some cases pedipalp-to-leg transformations. In more strongly affected embryos, adjacent appendages undergo fusion and/or truncation, and legs display proximal defects, suggesting conservation of additional functions of *hth* in patterning the antero-posterior and proximo-distal appendage axes. Expression signal of anterior Hox genes *labial*, *proboscipedia* and *Deformed* is diminished, but not absent, in *hth* RNAi embryos, consistent with results previously obtained with the insect *G. bimaculatus*. Our results substantiate a deep homology across arthropods of the mechanism whereby cephalic appendages are differentiated from locomotory appendages.

1. Introduction

One of the defining hallmarks of arthropod diversity is morphological disparity of the appendages. The diversification of arthropod appendages has transformed the evolutionary adaptive landscape for Arthropoda, unlocking access to various ecological opportunities and environments [1,2]. The fossil record and phylogeny of Arthropoda indicate that by the Early Cambrian, crown-group arthropods bore a division between cephalic, or 'head', appendages, and polyramous locomotory appendages on a homonomous 'trunk'. This division between cephalic and locomotory appendage-bearing segments is observed in such iconic Palaeozoic lineages as trilobites and 'great-appendage' arthropods (e.g. *Anomalocaris*), as well as Onychophora, the sister group of Arthropoda [3,4].

The segmental correspondence of anterior appendages, the ganglia of the arthropod tripartite brain and the anterior tagma has long been disputed [3,5–8]. A general consensus has formed that the first appendage-bearing

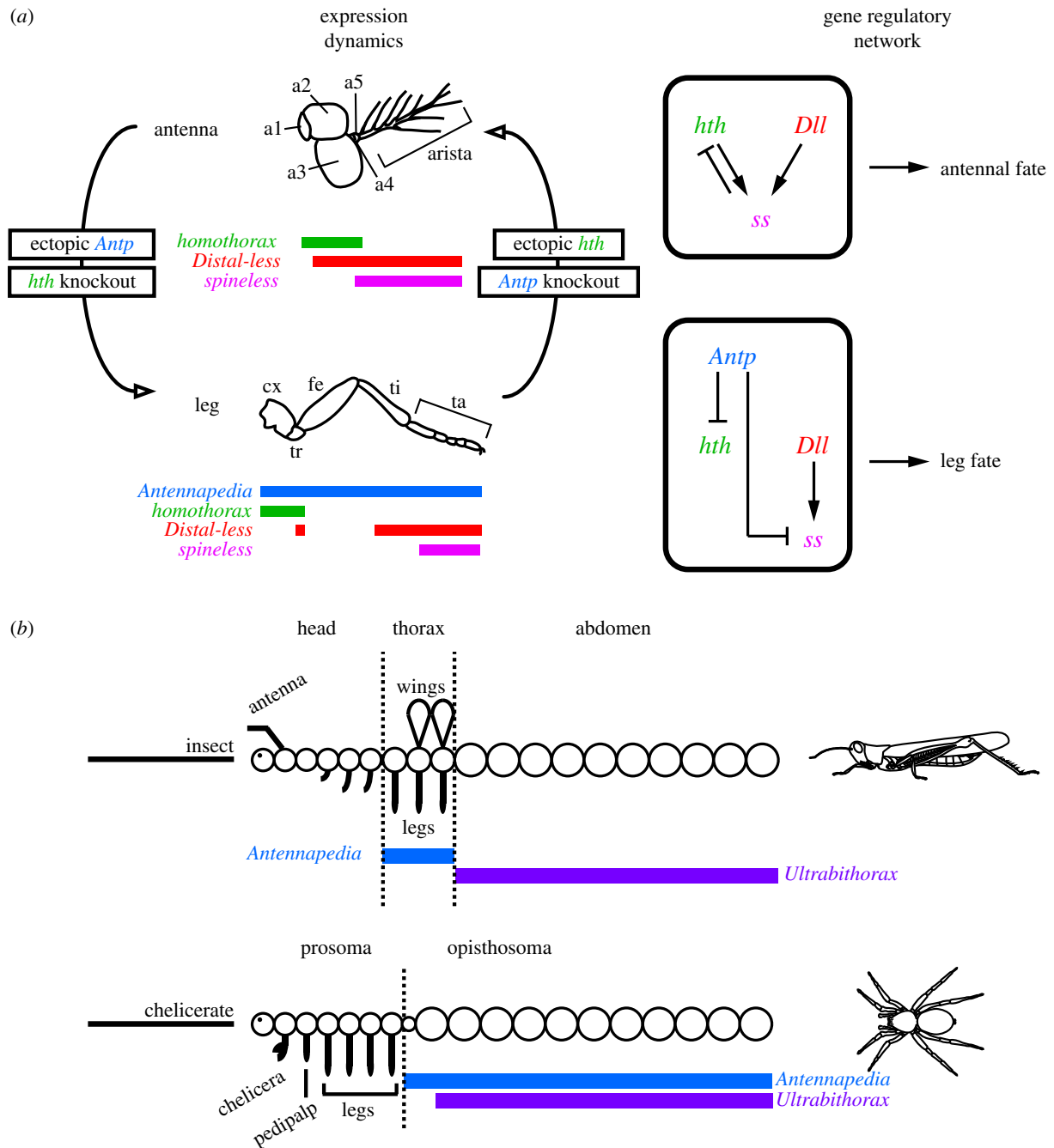


Figure 1. Developmental dynamics of *hth* expression in deuterocerebral and locomotory appendages. (a) Expression domains of *Antp*, *hth*, *Dll* and *ss* in the antenna and walking leg of *D. melanogaster*. In the antenna, *hth* knockdown or *Antp* overexpression results in antenna-to-leg transformation. In the leg, *hth* overexpression or *Antp* knockdown results in leg-to-antenna transformation. Gene interactions are shown to the right. (b) Comparative gene expression patterns of the Hox genes *Antp* and *Ubx* in an archetypal insect and arachnid. Note that chelicerate *Antp* is not expressed in the leg-bearing segments. (Online version in colour.)

segments of Mandibulata and Chelicerata are homologous, based both on the innervation of these appendages by the deuterocerebral ganglia (the second part of the tripartite arthropod brain), and on the absence of Hox gene expression in the deuterocerebral segment across arthropods [6,7,9–11]. Implicit in this homology statement is the homology of the deuterocerebral appendages, which are markedly different in both morphology and function between mandibulates and chelicerates. The deuterocerebral appendage of mandibulates (hexapods, crustaceans and myriapods) is invariably an antenna, which is typically elongate, composed of numerous segments ('antennomeres') and dedicated to sensory function. By contrast, the deuterocerebral appendage of chelicerates (pycnogonids, horseshoe crabs and arachnids) is the chelicera or chelifore, a short appendage consisting of two to four segments and involved in feeding.

Whereas the correspondence of arthropod head segments has a basis in neuroanatomical and developmental genetic evidence [6–11], the correspondence of antennae and chelicerae remains unsubstantiated.

The best understood case of deuterocerebral appendage fate specification is that of antennae in the fruit fly *Drosophila melanogaster* (figure 1). The Hox gene *Antennapedia* (*Antp*) is required for leg identity in the thorax, where *Antp* represses expression of the TALE-class gene *homothorax* (*hth*). This repression ensures that expression of *hth* in the outer margin of the developing leg discs (which patterns proximal podomeres [leg segments]) has minimal overlap with that of *Distal-less* (*Dll*, which patterns distal podomeres); the proximally restricted co-expression of *hth* and its cofactor *extradenticle* (*exd*) functions to pattern proximal podomeres. Knockdown of *Antp* (or

alternatively, ectopic expression of *hth* in the legs) results in leg-to-antenna transformation in the thorax [12–17]. Inversely, ectopic expression of *Antp* in the antennal disc, where it is normally not expressed (or alternatively, knockdown of antennal *hth* expression) causes antenna-to-leg transformations [15–17]. The repressive interaction between *hth* and *Antp* has been presumed to be direct (but see [18]). In addition, the selector gene *spineless* (*ss*), which acts downstream of *Antp*, *Dll* and *hth/exd*, confers distal antennal identity in the antenna (figure 1). In two holometabolous insect orders (*D. melanogaster* and four species of the beetle genus *Tribolium*), antennal *ss* expression arises within the *Dll* domain upon co-activation by *hth/exd* and *Dll*. At later stages, *ss* represses expression of *hth* in the distal tip of the antenna [14,19–21]. It has also been demonstrated that *Antp* represses *ss* in the legs directly, by competing with *Dll* for binding of the *ss* enhancer [18].

The similarity of the loss-of-function phenotypes of both *hth* and its cofactor *extradenticle* (*exd*) indicates that the Hox-binding Hth/Exd heterodimer fulfils multiple roles during patterning of both body and appendage axes [15,16,22]. Loss-of-function mutants of both *hth* and *exd* display: (i) segmentation defects along the antero-posterior axis of the body; (ii) proximal defects along the proximo-distal axis of appendages; and (iii) antenna-to-leg transformations.

Elements of the fruit fly-based antennal specification model (figure 1a) have been validated in three other insects [23–26]. Intriguingly, RNAi-mediated knockdown of *hth* in the cricket *Gryllus bimaculatus* causes all cephalic appendages, not just antennae, to transform towards leg identity [26]. Barring insects, functional data for arthropod *hth* are unavailable for all other lineages in the arthropod tree of life.

In Chelicerata, the sister group to the remaining Arthropoda, gene expression data for the *Antp* orthologue demonstrate conserved expression throughout the posterior tagma (opisthosoma) of multiple surveyed species, but absence from the leg-bearing prosoma [9,27–29], suggesting that chelicerate *Antp* is not involved in appendage identity specification (figure 1b). Concordantly, functional data have demonstrated that the spider *Antp* orthologue represses limb development in the opisthosoma of *Parasteatoda tepidariorum* [30]. By contrast, expression dynamics of *hth* are more comparable to insect counterparts. In chelicerates, *hth* is expressed throughout the developing limb buds in early stages of embryonic development, but retracts from the distal-most parts of the appendages in later stages [31,32], as in the antennal disc of *D. melanogaster* [15,16] (figure 2). In late states of chelicerate development, the degree of overlap between *hth* and *Dll* expression domains is unique to each appendage type [31,32]. As in *D. melanogaster*, this overlap is nearly complete in the deutocerebral appendages, but not in the walking legs, where *hth* is absent from the two distal-most podomeres [31–33] (figure 2).

This similarity of expression dynamics suggests that chelicerate *hth* has a function in specifying appendage identity. Therefore, we investigated the function of *hth* in the harvestman *Phalangium opilio*. We hypothesized that if patterning of the antenna and chelicera is homologous, then knockdown of *Po-hth* should result in a chelicera-to-leg homeotic transformation (as observed for insect *hth* knockdowns [13,16,19,24,26]). In support of this hypothesis, here we show that RNAi-mediated knockdown of the single-copy *hth* orthologue of *P. opilio* results in the same range of *hth* loss-of-function phenotypes observed in insects, and specifically includes homeotic transformation of chelicerae and pedipalps

towards leg identity. These data indicate that the mechanism of deutocerebral appendage fate specification is conserved in Chelicerata, and by extension, putatively across Arthropoda.

2. Material and methods

(a) Animal cultivation and gene cloning

Embryos of wild caught *P. opilio* and *Centruroides sculpturatus* were obtained as described previously [29,34]. Embryos of *Limulus polyphemus* were kindly provided by B. Battelle and H. J. Brockmann (Department of Biology, University of Florida) and were staged according to [35]. Isolation of the *P. opilio hth* fragment from a developmental transcriptome was previously reported [36]. We similarly isolated *hth* and *Dll* orthologues of *C. sculpturatus* from its corresponding developmental transcriptome [34]. Both fragments were cloned and Sanger sequenced for verification of transcriptomic assembly. PCR products were cloned using the TOPO[®] TA Cloning[®] Kit with One Shot[®] Top10 chemically competent *Escherichia coli* (Invitrogen, Carlsbad, CA, USA), following the manufacturer's protocol, and their identities verified by sequencing. Two non-overlapping *Po-hth* fragments of approximately similar size (286 bp and 299 bp) were separately amplified and cloned using internal primer pairs.

The *hth* orthologue from *L. polyphemus* was identified from NCBI expressed sequence tags databases using tblastx. Primers were designed to amplify an approximately 500 bp fragment that was then cloned by RT-PCR using cDNA from stage 19 to 20 embryos and Sanger sequenced to verify identity.

All primer sequences are provided in the electronic supplementary material, table S2. All verified *hth* sequences were accessioned in GenBank (KP129111–129113).

(b) Fixation and whole mount *in situ* hybridization of chelicerate embryos

Whole mount *in situ* hybridization was performed as previously described for *P. opilio* [28], *C. sculpturatus* [34] and *L. polyphemus* [37]. Riboprobe synthesis for *hth* and Hox genes also followed the respective published protocols. Embryos were mounted in glycerol and images were captured using an HrC AxioCam and an Axio Zoom V.16 fluorescence stereomicroscope driven by Zen (Zeiss).

(c) Double stranded RNA synthesis

Double stranded RNA (dsRNA) was synthesized with the MEGA-script[®] T7 kit (Ambion/Life Technologies, Grand Island, NY, USA) from amplified PCR product (above), following the manufacturer's protocol. The synthesis was conducted for 4 h, followed by a 5 min cool-down step to room temperature. A LiCl precipitation step was conducted, following the manufacturer's protocol. dsRNA quality and concentration were checked using a Nanodrop-1000 spectrophotometer (Thermo Scientific, Wilmington, DE, USA) and the concentration of the dsRNA was subsequently adjusted to 3.75–4.00 mg ml⁻¹.

(d) Embryonic RNA interference

Embryos of *P. opilio* were collected from wild caught females maintained in the laboratory. Embryos were dechorionated, dehydrated for 30 min and mounted on glass coverslips as described previously [38]. Eggs from each *P. opilio* clutch were randomly divided into control (20–30% of individuals) and *hth*-dsRNA injection treatments (70–80% of individuals).

As controls, 161 embryos were injected with exogenous dsRNA (a 678 bp fragment of *DsRed*) following a published protocol [38]. Animals were subsequently scored as wild-type (normal development), or as dead/indeterminate ('indeterminate'

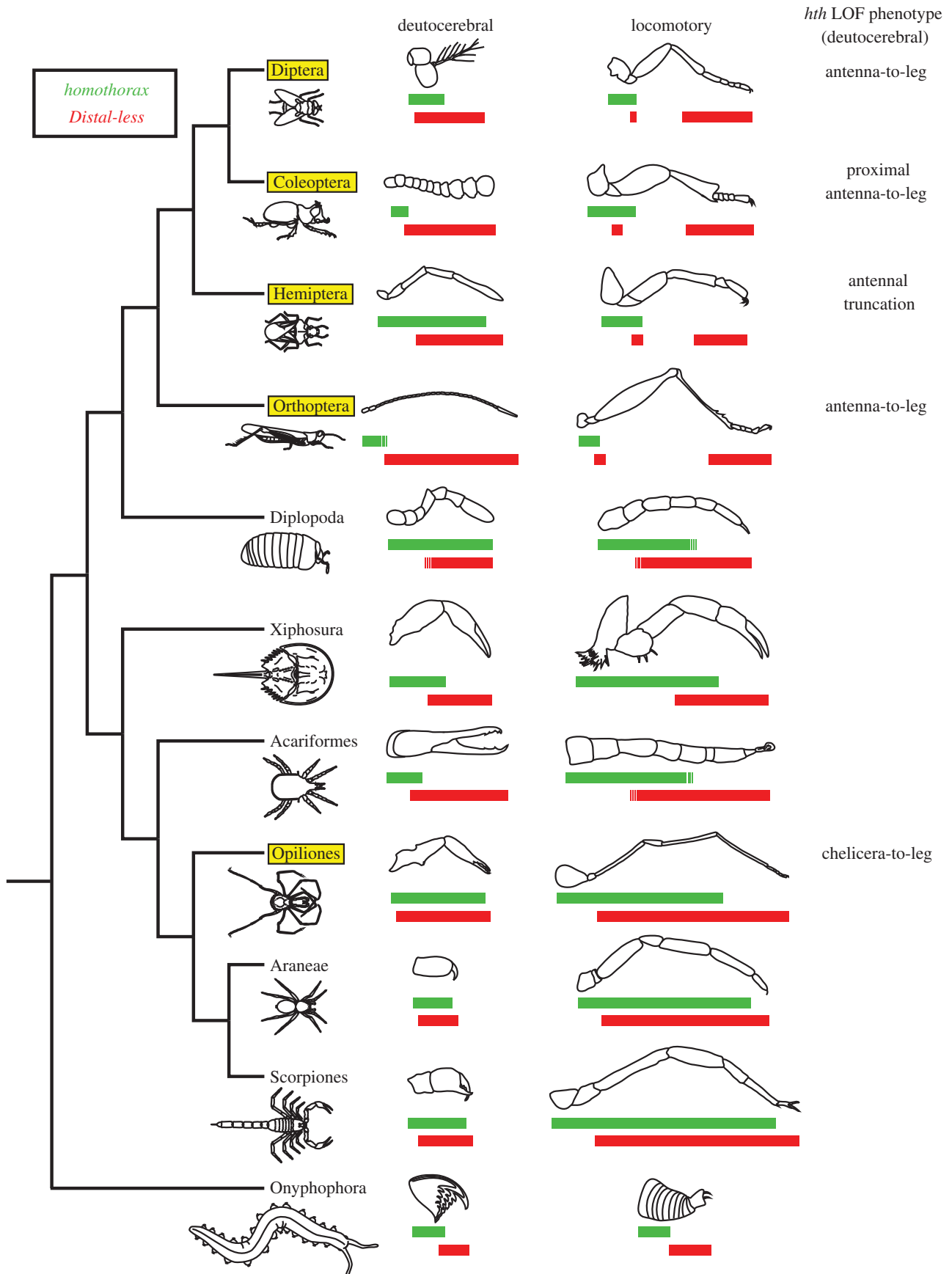


Figure 2. Reported expression boundaries of *hth* (green; upper bar) and *Dll* (red; lower bar) for deuto-cerebral and walking leg appendages across Arthropoda. Broken lines indicate uncertainty of expression boundary with respect to specific podomeres. Boxed orders indicate availability of functional data for *hth* orthologues (including from this study). References provided in the electronic supplementary material. (Online version in colour.)

indicates failure to complete development after six weeks post-injection and is typically accompanied by abnormal development at the site of injection). Results of injections are shown in the electronic supplementary material, figure S1 and table S1.

Another 256 embryos were injected with a 768 bp fragment of *hth*-dsRNA. Resulting embryos were classified into wild-type, dead/indeterminate, Class I (strong) phenotype (animals with defects in neurogenesis, anteroposterior (AP) segmentation,

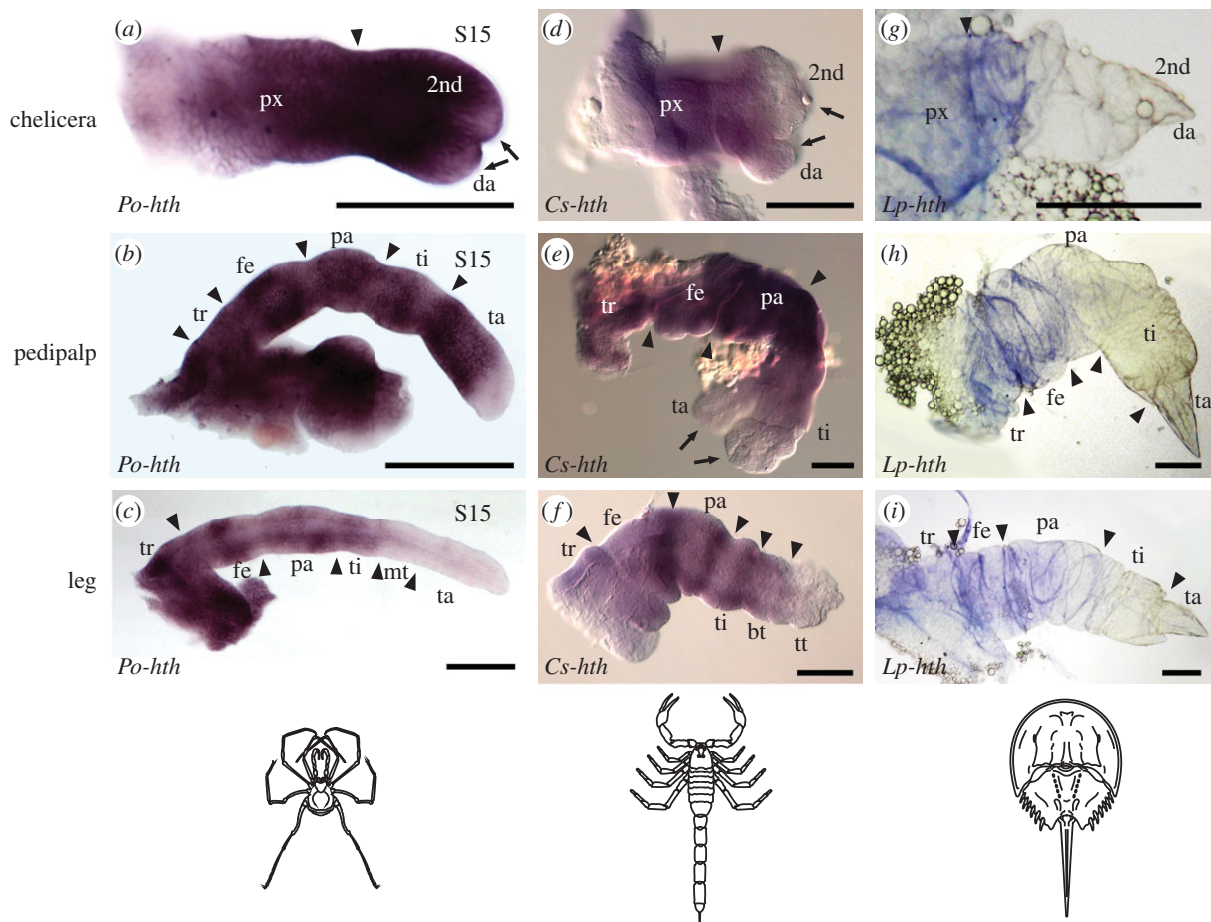


Figure 3. *hth* expression patterns in embryonic appendages of (a–c) the harvestman, *P. opilio*; (d–f) the scorpion, *C. sculpturatus*; and (g–i) the horseshoe crab, *L. polyphemus*. Arrowheads indicate segmental boundaries. Note absence of *hth* expression from both termini of all chelate appendages (arrows). Expression data for multiple spider species are closely comparable with harvestman counterparts and are not shown (figure 2). Scale bars, 100 μm . bt, basitarsus; da, distal article; fe, femur; mt, metatarsus; pa, patella; px, proximal segment; ta, tarsus; ti, tibia; tr, trochanter; tt, telotarsus. Expression data for *Dll* of *C. sculpturatus* are provided as the electronic supplementary material, figure S4. (Online version in colour.)

truncated appendages and severe proximal leg defects) and Class II (weak) phenotype (animals with proximal leg defects, homeotic transformation of gnathal appendages to legs or non-chelate chelicerae without homeotic transformation).

To exclude off-target effects caused by dsRNA injection, two additional and non-overlapping fragments of *Po-hth* (248 bp and 259 bp) were injected independently into 95 embryos each (electronic supplementary material, figure S1). Resulting embryos were classified the same way.

3. Results and discussion

(a) Podomeric boundaries of *homothorax* expression are conserved in Arachnida

Patterns of gene expression in Mandibulata have revealed that the proximal boundary of *hth* expression is variable in the deutocerebral antenna. Despite functional correspondence with *D. melanogaster* and *P. opilio* *hth* orthologues, *hth* expression in the cricket *G. bimaculatus* is proximally restricted in the antenna [26], whereas *hth* expression in the hemipteran *Oncopeltus fasciatus* spans nearly all of its antenna [24] (figure 2). Therefore, to infer whether any putative role of *hth* identified in *P. opilio* is generalizable to other members of Chelicerata, we took two approaches. First, we surveyed the literature for known expression patterns of *hth* in chelicerates (e.g. spiders;

[32,33]). Second, we generated novel *hth* expression data for the chelicerates *C. sculpturatus* (scorpion) and *L. polyphemus* (horseshoe crab).

Our *in situ* hybridization experiments revealed that in contrast to mandibulates, distal expression boundaries of all arachnid *hth* orthologues examined were similar in stages wherein podomeres are recognizable (figure 3). Nearly ubiquitous and strong expression of *hth* occurred in chelicerae of Arachnida, except in the distal-most parts of the chela. In posterior appendages, *hth* expression domains also occurred broadly throughout the appendage, as in *P. opilio*. By contrast, *hth* expression in *L. polyphemus* extended only to the proximal part of the secondary article of the chelicerae, and the proximal part of the tibia of posterior appendages (figure 3). This difference may be attributable to stage incompatibilities between *L. polyphemus* and the arachnids, as horseshoe crabs undergo a series of embryonic moults with concomitant saltational morphogenesis that is not observed in Arachnida [35]. Absence of (or weaker) *hth* expression was observed in the distal tips of all chelate appendages, suggesting that the chela constitutes a distal bifurcation of the proximodistal (PD) axis throughout Chelicerata.

Based upon the data presented here, taken together with reported expression patterns in the millipede *Glomeris marginata* and multiple spider species [32,33], we infer that broad expression of *hth* and *Dll* in both proximal and distal territories of deutocerebral appendages was present in the arthropod

common ancestor. The ancestral state of gene expression in the common ancestor of Panarthropoda remains ambiguous, as *hth* and *Dll* expression in the unsegmented deutocerebral appendage (jaw) of Onychophora is different from that of basal arthropods (figure 2).

(b) A conserved pleiotropic spectrum of *homothorax* phenotypes in insects and *Phalangium opilio*

In situ hybridizations for *hth* on embryos with strong *hth* loss-of-function phenotypes showed decreased *hth* expression in wild-type domains (electronic supplementary material, figure S2), confirming effective RNAi-mediated knockdown of *hth* expression. Of the 202 embryos surviving injection of *hth*-dsRNA, 22% ($n = 45$), displayed developmental defects including antero-posterior segmental fusions in the prosoma, proximal leg defects and/or homeotic transformation of gnathal appendages. We classified embryos with antero-posterior segmental fusions and/or whole-appendage truncations as Class I (strong) phenotypes ($n = 21$), and embryos with proximal leg defects and/or homeotically transformed appendages as Class II (weak) phenotypes ($n = 24$). Mosaic phenotypes, wherein loss-of-function defects were observed principally in only one-half of the embryo, occurred in 43% of Class I ($n = 9$) and 100% of Class II ($n = 24$) phenotypes. This range of phenotypes was observed upon injection of a 768 bp fragment of *hth*-dsRNA, and either of two non-overlapping fragments amplified from the same *Po-hth* clone (248 and 259 bp; electronic supplementary material, table S1 and figure S1), confirming specificity of these *hth* knockdown phenotypes.

Embryos with Class I phenotypes (electronic supplementary material, figure S2) did not survive to hatching. Head patterning defects included partial or complete loss of the head lobe. Embryos in this phenotype class displayed fusions of adjacent segments along the AP axis, typically the cheliceral and pedipalpal segments. The labrum and/or some appendages also failed to form. When present, appendages were fused or showed proximal patterning defects, with proximal podomeres and endites failing to form (electronic supplementary material, figure S2). We interpret these phenotypes to be highly comparable with the AP segmentation defects and PD proximal patterning defects observed upon knockdown of *hth* in insects [24,26].

In contrast to all Class I phenotype embryos, some mosaic Class II phenotype embryos (figure 4) survived to hatching, enabling morphological corroboration of homeosis. In some embryos with Class II phenotypes ($n = 7$), a tarsus-like structure with a single terminal claw and leg-like setation patterns formed in place of the chela, indicating homeotic transformation to leg identity (figure 4g). In embryos with more severe Class II phenotypes ($n = 13$), distal elements of both chelicera and pedipalp were transformed towards leg-like identity, as inferred from podomeres with leg-like setation patterns and absence of pedipalpal spurs (figure 4h).

The harvestman *hth* knockdown appendage phenotypes described above are remarkably similar to those observed in insects. Among hemimetabolous insects, in the cricket *G. bimaculatus*, parental RNAi-mediated knockdown of *hth* resulted in similar transformation of all cephalic appendages towards leg identity in some embryos, and comparable fusion of adjacent segments in stronger phenotypes [26]. In parental RNAi experiments with the milkweed bug *O. fasciatus*, weaker *hth* phenotypes consisted of distal labium (second

maxilla)-to-leg transformations, and truncation of antennae [24]. The similar range of phenotypes observed upon knockdown of *hth* orthologues in multiple insects and the chelicerate exemplar *P. opilio* suggests evolutionary conservation of *hth* function in proximo-distal patterning and cephalic appendage specification over 550 million years of arthropod evolution. The implicit serial homology of antennae and chelicerae is consistent with transitional morphologies observed in the fossil record, such as the antenniform chelicerae of the Silurian synziphosurines *Dibasterium durgae* and *Offacolus kingi* [39,40]. The unique deutocerebral appendages of these stem-horseshoe crabs elude facile characterization, as they are interpreted to bear a large number of articulated segments (typical of antennae) and also a distal chela composed of two segments (typical of chelicerae). Similar comparisons have also been made between modern chelicerae and a series of 'great-appendage' arthropod fossils [8,41], and particularly so for the reconstructed deutocerebral appendages of leanchioliids that exemplify the intermediate condition of chelicerae (three distal axes, dentition) and antennae (three flagella with numerous antennules) [42]. Taken together with the absence of Hox gene expression in the deutocerebral segment of all surveyed panarthropods [6,10,43], as well as the conservation of *hth* function in insects and a chelicerate (this study), the existence of such transitional morphologies in the fossil record suggests that different aspects of the ancestral deutocerebral appendage were retained by the mandibulate and chelicerate lineages. The morphological distinction between antenna and chelicera may thus result from differential losses of downstream targets of *hth* that occurred in a lineage-specific manner. The role of *ss* as one such downstream target of *hth* is currently under investigation in chelicerates (P. P. Sharma, W. C. Wheeler and C. G. Extavour 2015, personal communication).

With respect to conservation of gene interaction, knockdown of the *hth* cofactor *exd* in *G. bimaculatus* results in similar homeotic transformation of gnathal appendages towards leg identity, with accompanying loss of gnathal Hox gene expression (*Deformed* and *Sex combs reduced*; [25]). The similar phenotypes resulting from knockdown of either *hth* or *exd* reflect the requirement of Hth for transport of Exd to the nucleus, and the instability of Hth in the absence of Exd [22,44]. However, knockdown of *hth* in *G. bimaculatus* does not eliminate anterior Hox gene expression, in contrast to knockdown of *exd* in the same species [25,26]. Comparably, we observed diminished, but not eliminated, expression of the Hox genes *labial*, *proboscipedia*, or *Deformed* in Class I *P. opilio* embryos (electronic supplementary material, figure S3).

This finding is suggestive of a conserved, if poorly understood, mechanism whereby *hth* interacts with Hox genes, such that cephalic appendage identities are specified by varying *hth* expression, as determined by Hox input [26]. Indeed, Hth and Exd are *bona fide* Hox cofactors in *D. melanogaster* [22,44–46]. However, functional data for chelicerate Hox genes are limited to analysis of *Antp*, and thus the interaction of *hth* and anterior Hox genes is unknown for chelicerates [30]. In addition, *Antp* in the spider *P. tepidariorum* appears to have a function that is convergent upon the role of *Ultrabithorax* in insects (i.e. repressing appendage formation), suggesting that Hox function in appendage-bearing segments of mandibulates and chelicerates is not directly comparable (figure 1). An alternative interpretation of the cricket and harvestman data may also be that *hth* RNAi phenotypes are generally weaker than *exd* RNAi phenotypes, and that

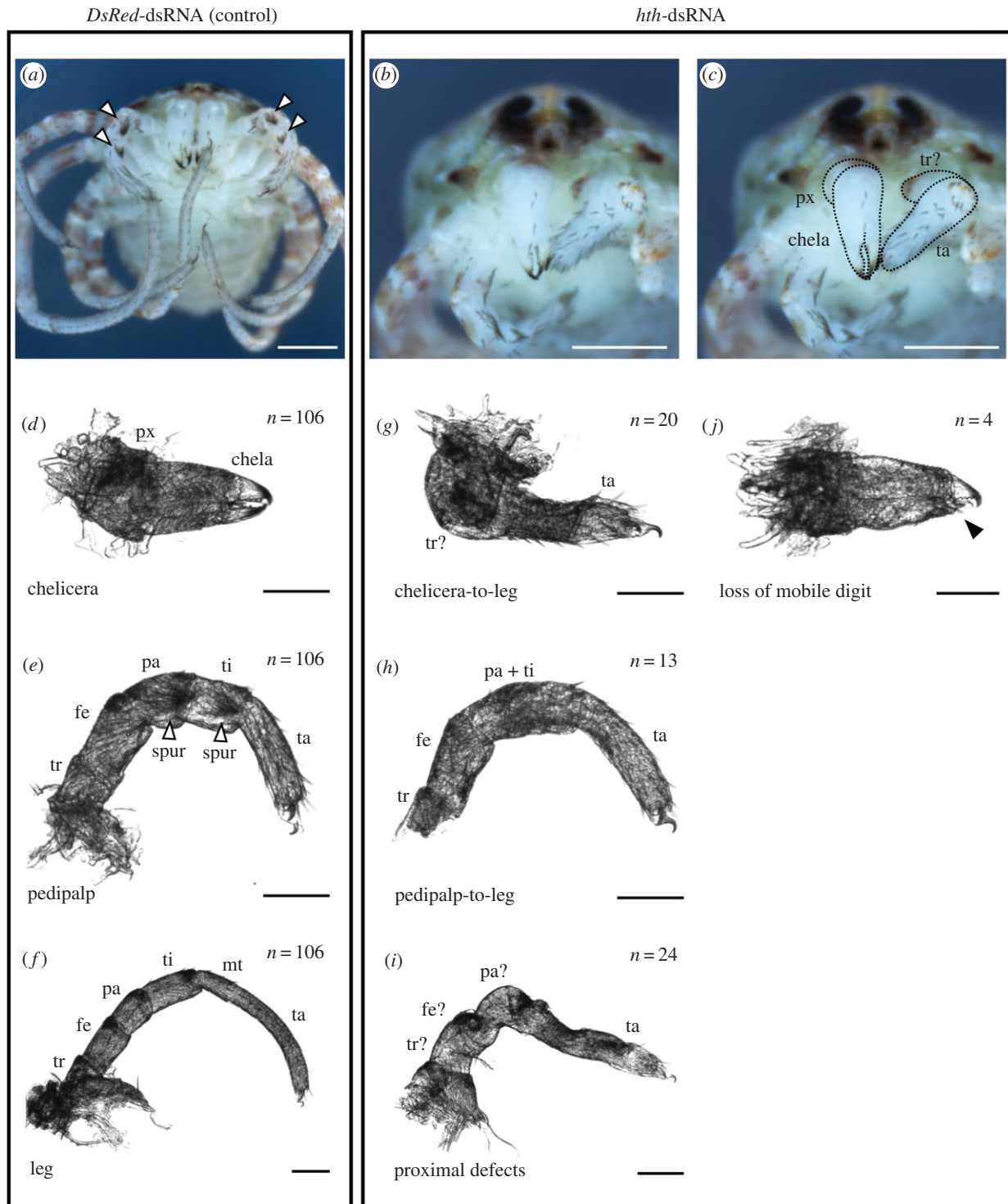


Figure 4. Knockdown of *hth* results in homeotic transformations of gnathal appendages to legs in a chelicerate (Class II phenotype). (a) Control-injected hatchling of *P. opilio*, demonstrating wild-type morphology (ventral view). White arrowheads indicate pedipalpal spurs, which distinguish these appendages. (b,c) *hth-dsRNA*-injected hatchling of *P. opilio* in ventral view, exhibiting homeotic chelicera-to-leg transformation on one side (animal's left). (c) Same figure as in (b), with deutocerebral appendages outlined for clarity. (d–f) Appendage mounts of control-injected hatchlings. White arrowheads in (e) indicate pedipalpal spurs. (g–j) Appendage mounts of *hth-dsRNA*-injected hatchlings. Homeotic chelicera-to-leg transformation (g) and pedipalp-to-leg transformation (h) are accompanied by proximal leg defects (i). Note absence of pedipalpal spurs in (h). (j) Loss of mobile digit in a chelicera (black arrowhead). Scale bar for (a–c): 200 μm . Scale bar for (d–j): 50 μm . Abbreviations as in figure 3. (Online version in colour.)

eliminating *hth* expression would result in loss of Hox expression in both species [26].

(c) A possible role for *homothorax* in patterning terminal chelae

An outstanding question regarding the evolution of the arthropod appendage is the mechanism whereby chelate

appendages acquired a chela, i.e. a distal bifurcation of the PD axis. In the spectrum of *hth* knockdown phenotypes in *P. opilio*, we observed that in the weakest of the Class II phenotypes ($n = 4$), the chelicerae retained dentition and cheliceral setation (i.e. retained cheliceral identity), but the mobile digit (i.e. distal article) was reduced (figure 4j). In the *P. opilio* chela, the mobile digit is the smaller of two distal buds that strongly expresses *hth* prior to segmentation.

One possible mechanism for the bifurcation of the distal cheliceral limb bud is recruitment of *hth* itself for patterning this secondary axis. Overexpression of *hth* in *D. melanogaster* results in just such a duplication of the antennal axis at the a3 segment [47]. Together with similar expression patterns of *hth* in other chelate appendage termini, these data suggest a common mechanism whereby chelae are formed in various arthropod appendages. Beyond RNAi approaches in scorpions (chelate chelicerae and pedipalps), horseshoe crabs (all prosomal appendages chelate) or such mandibulates as pauropods (bifurcating antennae), this hypothesis could also be tested in future through misexpression of *hth* in non-chelate appendages of emerging model chelicerates like the spider *P. tepidariorum*, with the prediction that ectopic *hth* expression would cause distal axis duplication in the pedipalps and legs (as in *D. melanogaster*). At present, such functional tools are presently not available for chelicerates, being limited to RNAi in spiders, mites and harvestmen.

4. Conclusion

Our results reveal an ancestral mechanism whereby cephalic and locomotory appendages are differentiated in arthropods. RNAi-mediated gene knockdown of a chelicerate *hth* orthologue demonstrates extraordinary conservation of multiple

functions, including specification of gnathal appendage identity and proximo-distal axial patterning. The transformation of both the antenna and the chelicera towards leg identity upon knockdown of *hth*, together with the absence of any Hox gene expression in their respective segments, is consistent with the serial homology of deutocerebral appendages. Future investigations should emphasize identification of lineage-specific (i.e. antennal versus cheliceral) deutocerebral selector genes, towards testing the hypothesis that variation in deutocerebral appendage morphology is attributable to evolution in the downstream targets of *hth*.

Acknowledgements. Douglas Richardson facilitated imaging at the Harvard Center for Biological Imaging. Discussions with David R. Angelini, Frank W. Smith and Gonzalo Giribet refined some of the ideas presented in this study. Comments from Associate Editor Philip Donoghue and two anonymous reviewers improved an earlier draft of the manuscript.

Funding statement. This work was partially supported by NSF grant no. IOS-1257217 to C.G.E. and AMNH funds to W.W. P.P.S. was supported by the National Science Foundation Postdoctoral Research Fellowship in Biology under grant no. DBI-1202751.

Authors' contributions. P.P.S. conceived of the project, designed the study, collected arachnid data and wrote the manuscript. P.P.S. and E.E.S. jointly analysed RNAi data. O.A.T. and D.H.L. collected horseshoe crab data. M.J.C., W.C.W. and C.G.E. provided resources and funding for various parts of the study. All authors edited the manuscript and approved the final content.

References

- Snodgrass RE. 1938 Evolution of the Annelida, Onychophora and Arthropoda. *Smithson. Misc. Coll.* **97**, 1–159.
- Boxshall GA. 2004 The evolution of arthropod limbs. *Biol. Rev.* **79**, 253–300. (doi:10.1017/S1464793103006274)
- Budd GE. 2002 A palaeontological solution to the arthropod head problem. *Nature* **417**, 271–275. (doi:10.1038/417271a)
- Waloszek D, Chen J, Maas A, Wang X. 2005 Early Cambrian arthropods: new insights into arthropod head and structural evolution. *Arthropod Struct. Dev.* **34**, 189–205. (doi:10.1016/j.asd.2005.01.005)
- Maxmen A, Browne WE, Martindale MQ, Giribet G. 2005 Neuroanatomy of sea spiders implies an appendicular origin of the protocerebral segment. *Nature* **437**, 1144–1148. (doi:10.1038/nature03984)
- Jager M, Muriene J, Clabaut C, Deutsch J, Le Guyader H, Manuel M. 2006 Homology of arthropod anterior appendages revealed by Hox gene expression in a sea spider. *Nature* **441**, 506–508. (doi:10.1038/nature04591)
- Scholtz G, Edgecombe GD. 2006 The evolution of arthropod heads: reconciling morphological, developmental and palaeontological evidence. *Dev. Genes Evol.* **216**, 395–415. (doi:10.1007/s00427-006-0085-4)
- Tanaka G, Hou X, Ma X, Edgecombe GD, Strausfeld NJ. 2013 Chelicerate neural ground pattern in a Cambrian great appendage arthropod. *Nature* **502**, 364–367. (doi:10.1038/nature12520)
- Telford MJ, Thomas RH. 1998 Expression of homeobox genes shows chelicerate arthropods retain their deutocerebral segment. *Proc. Natl Acad. Sci. USA* **95**, 10 671–10 675. (doi:10.1073/pnas.95.18.10671)
- Hughes CL, Kaufman TC. 2002 Hox genes and the evolution of the arthropod body plan. *Evol. Dev.* **4**, 459–499. (doi:10.1046/j.1525-142X.2002.02034.x)
- Brenneis G, Ungerer P, Scholtz G. 2008 The chelifores of sea spiders (Arthropoda, Pycnogonida) are the appendages of the deutocerebral segment. *Evol. Dev.* **10**, 717–724. (doi:10.1111/j.1525-142X.2008.00285.x)
- Struhl G. 1982 Genes controlling segmental specification in the *Drosophila* thorax. *Proc. Natl Acad. Sci. USA* **79**, 7380–7384. (doi:10.1073/pnas.79.23.7380)
- Casares F, Mann RS. 1998 Control of antennal versus leg development in *Drosophila*. *Nature* **392**, 723–726. (doi:10.1038/33706)
- Duncan DM, Burgess EA, Duncan I. 1998 Control of distal antennal identity and tarsal development in *Drosophila* by *spineless*—*aristopedia*, a homolog of the mammalian dioxin receptor. *Genes Dev.* **12**, 1290–1303. (doi:10.1101/gad.12.9.1290)
- Dong PDS, Chu J, Panganiban G. 2001 Proximodistal domain specification and interactions in developing *Drosophila* appendages. *Development* **128**, 2365–2372.
- Dong PDS, Dicks JS, Panganiban G. 2002 *Distal-less* and *homothorax* regulate multiple targets to pattern the *Drosophila* antenna. *Development* **129**, 1967–1974.
- Emerald BS, Cohen SM. 2004 Spatial and temporal regulation of the homeotic selector gene *Antennapedia* is required for the establishment of leg identity in *Drosophila*. *Dev. Biol.* **267**, 462–472. (doi:10.1016/j.ydbio.2003.12.006)
- Duncan D, Kieffel P, Duncan I. 2010 Control of the *spineless* antennal enhancer: direct repression of antennal target genes by *Antennapedia*. *Dev. Biol.* **347**, 82–91. (doi:10.1016/j.ydbio.2010.08.012)
- Angelini DR, Kikuchi M, Jockusch EL. 2009 Genetic patterning in the adult capitate antenna of the beetle *Tribolium castaneum*. *Dev. Biol.* **327**, 240–251. (doi:10.1016/j.ydbio.2008.10.047)
- Shippy TD, Yeager SJ, Denell RE. 2009 The *Tribolium spineless* ortholog specifies both larval and adult antennal identity. *Dev. Genes Evol.* **219**, 45–51. (doi:10.1007/s00427-008-0261-9)
- Toegel JP, Wimmer EA, Prpic N-M. 2009 Loss of *spineless* function transforms the *Tribolium* antenna into a thoracic leg with pretarsal, tibiotarsal and femoral identity. *Dev. Genes Evol.* **219**, 53–58. (doi:10.1007/s00427-008-0265-5)
- Rieckhof GE, Casares F, Ryo HD, Abu-Shaar M, Mann RS. 1997 Nuclear translocation of *extradenticle* requires *homothorax*, which encodes an *extradenticle*-related homeodomain protein. *Cell* **91**, 171–183. (doi:10.1016/S0092-8674(00)80400-6)
- Smith FW, Angelini DR, Jockusch EL. 2014 A functional genetic analysis in flour beetles (Tenebrionidae) reveals an antennal identity specification mechanism active during metamorphosis in Holometabola. *Mech. Dev.* **132**, 13–27. (doi:10.1016/j.mod.2014.02.002)
- Angelini DR, Kaufman TC. 2004 Functional analyses in the hemipteran *Oncopeltus fasciatus* reveal

- conserved and derived aspects of appendage patterning in insects. *Dev. Biol.* **271**, 306–321. (doi:10.1016/j.ydbio.2004.04.005)
25. Mito T, Ronco M, Uda T, Nakamura T, Ohuchi H, Noji S. 2007 Divergent and conserved roles of *extradenticle* in body segmentation and appendage formation, respectively, in the cricket *Gryllus bimaculatus*. *Dev. Biol.* **313**, 67–79. (doi:10.1016/j.ydbio.2007.09.060)
 26. Ronco M, Uda T, Mito T, Minelli A, Noji S, Klingler M. 2008 Antenna and all gnathal appendages are similarly transformed by *homothorax* knock-down in the cricket *Gryllus bimaculatus*. *Dev. Biol.* **313**, 80–92. (doi:10.1016/j.ydbio.2007.09.059)
 27. Damen WGM, Hausdorf M, Seyfarth E-A, Tautz D. 1998 A conserved mode of head segmentation in arthropods revealed by the expression pattern of Hox genes in a spider. *Proc. Natl Acad. Sci. USA* **95**, 10 665–10 670. (doi:10.1073/pnas.95.18.10665)
 28. Sharma PP, Schwager EE, Extavour CG, Giribet G. 2012 Hox gene expression in the harvestman *Phalangium opilio* reveals divergent patterning of the chelicerate opisthosoma. *Evol. Dev.* **14**, 450–463. (doi:10.1111/j.1525-142X.2012.00565.x)
 29. Sharma PP, Schwager EE, Extavour CG, Wheeler WC. 2014 Hox gene duplications correlate with posterior heteronomy in scorpions. *Proc. R. Soc. B* **281**, 20140661. (doi:10.1098/rspb.2014.0661)
 30. Khadjeh S, Turetzek N, Pechmann M, Schwager EE, Wimmer EA, Damen WGM, Prpic N-M. 2012 Divergent role of the Hox gene *Antennapedia* in spiders is responsible for the convergent evolution of abdominal limb repression. *Proc. Natl Acad. Sci. USA* **109**, 4921–4926. (doi:10.1073/pnas.1116421109)
 31. Sharma PP, Schwager EE, Extavour CG, Giribet G. 2012 Evolution of the chelicera: a *dachshund* domain is retained in the deutocerebral appendage of Opiliones (Arthropoda, Chelicerata). *Evol. Dev.* **14**, 522–533. (doi:10.1111/ede.12005)
 32. Prpic N-M, Damen WGM. 2004 Expression patterns of leg genes in the mouthparts of the spider *Cupiennius salei* (Chelicerata: Arachnida). *Dev. Genes Evol.* **214**, 296–302. (doi:10.1007/s00427-004-0393-5)
 33. Pechmann M, Prpic N-M. 2009 Appendage patterning in the South American bird spider *Acanthoscurria geniculata* (Araneae: Mygalomorphae). *Dev. Genes Evol.* **219**, 189–198. (doi:10.1007/s00427-009-0279-7)
 34. Sharma PP, Gupta T, Schwager EE, Wheeler WC, Extavour CG. 2014 Subdivision of arthropod *cap-n-collar* expression domains is restricted to Mandibulata. *EvoDevo* **5**, 3. (doi:10.1186/2041-9139-5-3)
 35. Sekiguchi K, Yamamichi Y, Costlow JD. 1982 Horseshoe crab developmental studies. I. Normal embryonic development of *Limulus polyphemus* compared with *Tachypleus tridentatus*. *Prog. Clin. Biol. Res.* **81**, 53–73.
 36. Sharma PP, Kaluziak ST, Pérez-Porro AR, González VL, Hormiga G, Wheeler WC, Giribet G. 2014 Phylogenomic interrogation of Arachnida reveals systemic conflicts in phylogenetic signal. *Mol. Biol. Evol.* **31**, 2963–2984. (doi:10.1093/molbev/msu235)
 37. Blackburn DC, Conley KW, Plachetzki DC, Kempler K, Battelle BA, Brown NL. 2008 Isolation and expression of *Pax6* and *atonal* homologues in the American horseshoe crab, *Limulus polyphemus*. *Dev. Dyn.* **237**, 2209–2219. (doi:10.1002/dvdy.21634)
 38. Sharma PP, Schwager EE, Giribet G, Jockusch EL, Extavour CG. 2013 *Distal-less* and *dachshund* pattern both plesiomorphic and apomorphic structures in chelicerates: RNAinterference in the harvestman *Phalangium opilio* (Opiliones). *Evol. Dev.* **15**, 228–242. (doi:10.1111/ede.12029)
 39. Sutton MD, Briggs DEG, Siveter DJ, Siveter DJ, Orr PJ. 2002 The arthropod *Offacolus kingi* (Chelicerata) from the Silurian of Herefordshire, England: computer based morphological reconstructions and phylogenetic affinities. *Proc. R. Soc. Lond. B* **269**, 1195–1203. (doi:10.1098/rspb.2002.1986)
 40. Briggs DEG, Siveter DJ, Siveter DJ, Sutton MD, Garwood RJ, Legg D. 2012 Silurian horseshoe crab illuminates the evolution of arthropod limbs. *Proc. Natl Acad. Sci. USA* **109**, 15 702–15 705. (doi:10.1073/pnas.1205875109)
 41. Chen J, Waloszek D, Maas A. 2004 A new ‘great-appendage’ arthropod from the Lower Cambrian of China and homology of chelicerate chelicerae and raptorial antero-ventral appendages. *Lethaia* **37**, 3–20.
 42. Aria C, Caron J-B, Gaines R. 2015 A large new leanchoilid from the Burgess Shale and the influence of inapplicable states on stem arthropod phylogeny. *Palaeontology*. (doi:10.1111/pala.12161)
 43. Janssen R, Eriksson BJ, Tait NN, Budd G. 2014 Onychophoran Hox genes and the evolution of arthropod Hox gene expression. *Front. Zool.* **11**, 22. (doi:10.1186/1742-9994-11-22)
 44. Abu-Shaar M, Ryoo HD, Mann RS. 1999 Control of the nuclear localization of *extradenticle* by competing nuclear import and export signals. *Genes Dev.* **13**, 935–945. (doi:10.1101/gad.13.8.935)
 45. Ryoo HD, Mann RS. 1997 The control of trunk Hox specificity and activity by *extradenticle*. *Genes Dev.* **13**, 1704–1716. (doi:10.1101/gad.13.13.1704)
 46. Saadaoui M, Merabet S, Litim-Mecheri I, Arbeille E, Sambrani N, Damen W, Brena C, Pradel J, Graba Y. 2011 Selection of distinct Hox–*extradenticle* interaction modes fine-tunes Hox protein activity. *Proc. Natl Acad. Sci. USA* **108**, 2276–2281. (doi:10.1073/pnas.1006964108)
 47. Yao L-C, Liaw GJ, Pai CY, Sun YH. 1999 A common mechanism for antenna-to-leg transformation in *Drosophila*: suppression of *homothorax* transcription by four HOM-C genes. *Dev. Biol.* **211**, 268–276. (doi:10.1006/dbio.1999.9309)